MAX-PLANCK-INSTITUT FÜR PLASMAPHYSIK

GARCHING BEI MÜNCHEN

The very bright field ionization and field evaporation ion sources. Some uses. A beam formation and scanning system.

Die sehr hellen Feldionisations- und Feldverdampfungsionenquellen. Einige Anwendungen. Ein Strahl- und Ablenksystem.

H.Heil und R.Guckenberger

IPP 9/6 June 1972

Die nachstehende Arbeit wurde im Rahmen des Vertrages zwischen dem Max-Planck-Institut für Plasmaphysik und der Europäischen Atomgemeinschaft über die Zusammenarbeit auf dem Gebiete der Plasmaphysik durchgeführt.

IPP 9/6 June 1972
(In English)

The very bright field ionization and field evaporation ion sources. Some uses. A beam formation and scanning System.*

H.Heil and R.Guckenberger

Abstract

Field ionization and evaporation ion sources, in the form of small wire tips are capable of delivering brightnesses many orders of magnitude larger than conventional sources, with the apparent source size in the 10Å range. Therefore, they serve well as small ion probes for scanning instruments. These instruments, in turn, are unique in their ability to machine very small structures by sputtering, smaller than can be made by other means. Uses are in surface micro-analysis, microelectronics, electron and X-ray diffraction and manipulation and treatment of macromolecules. - For focusing, only electrostatic lenses can be used. Computations have shown the aperture lens to be far superior to the usual einzel lens with respect to smallness of focal length and spherical aberration constant. This advantage has to be weighed against the complication of having the target immersed into the electric field. We decided for this type of lens and describe the design of a scanning ion microscope which incorporates such a lens.

Zusammenfassung

Man kann von Feldionisations- und Feldverdampfungsionenquellen Richtstrahlwerte erhalten, die viele Größenordnungen größer sind als diejenigen der üblichen Ionenquellen, wobei die wirksamen Quellengrößen um 10Å liegen. Deshalb sind solche Quellen wohl geeignet für kleine Ionensonden für Rasterinstrumente.

Mit solchen Instrumenten kann man dann durch Zerstäubung Strukturen fräsen bis zu Dimensionen von einigen 10Å. Anwendungen liegen in der Oberflächenmikroanalyse, Mikroelektronik, Elektronen- und Röntgenbeugung und Behandlung von Makromolekülen. - Zum Fokussieren können nur elektronische Linsen benutzt werden. Als solche hat die Aperturlinse sich als weit überlegen gezeigt, bezüglich Kleinheit der Brennweite und sphärischen Aberrationskonstanten. Dieser Vorteil steht dem Nachteil gegenüber, daß das Target sich im vollen elektrischen Feld befindet. Wir haben uns für die Benützung dieser Linse entschieden und beschreiben die Konstruktion eines Rasterionenmikroskopes, das mit dieser Linse arbeitet.

---

*Die nachstehende Arbeit gibt eine Reproduktion eines Vortrages, der am 20. Oktober 1971 in dem "Symposium on Ion Sources and Formation of Ion Beams" im "Brookhaven National Laboratory" gehalten wurde. - Die Arbeit ist erschienen in den "Proc. Symp. on Ion Sources and Formation of Ion Beams, p.183, BNL 50310, editor: Th.J.M.Sluyters, Brookhaven National Laboratory, Upton, N.Y.".

I. Introduction

The ion sources which are the subject of this paper are of a different kind. They produce small currents in the range from pA to nA. There is no high power dissipation and associated difficulties with high temperatures and material failures. Less than a mW is dissipated in the source. The virtues of these sources rest in a 10^3 to 10^6 times higher brightness and in the extremesmallness of the apparent source of about 10 Å in diameter.

In order to work on such a new application of field ionization (FI) or field evaporation (FE), it is necessary esp. nowadays, to show its usefulness or relevance. Here is what we can list.

The commercially available scanning ion microscope or the ion microprobe[1] uses a duoplasmatron source. For it, one would like to have scanning ion spots smaller than the present lower limit of 1μm while maintaining a spot current of 10^{-10} A, one would like to have the source small enough to be able to focus with one single lens instead of the two-stage demagnifying optic, one would like to have the source clean enough to be able to dispense with the mass separation of the primary beam, and one would like to have the power input to the source low enough to facilitate the maintenance of an ultra high vacuum at the target.

In making masks for microelectronics one strives for ever smaller structures and has reached the limit set by the wavelength of light for photoformed masks and by the scattering depth of electrons for electron-beam-formed masks. Ion probes can be made smaller, penetrate far less, and remove material by sputtering without local heating.

The making of submicroscopic structures is also usefull for echelette gratings for UV and X-ray, as well as gratings and

Fresnel lenses for diffraction of electrons. - In biological applications, one can make microsieves with high throughput to separate macromolecules according to size. One may even consider placing an appropriate mask over a biological specimen in the electronmicroscope, align it to a certain spot on the specimen, and cut into that spot with flooding ion beam or make a deposit onto that spot with a vapor beam. - Thus, the sources are not only interesting physics, but also useful as a new technology.

In the past year in Munich, we have constructed such a scanning ion microscope. Much of the ion optical design and detection system is rather novel.

In the following we discuss the three optical arrangements which were considered:
First, an all-electrostatic gun, as reported by A.V.Crewe et al.[2], with a field emitter, a special accelerating lens, a scanning system, and the target.
Second, a system with electrostatic deflection prior to the final lens, which is an aperture lens with the target in the electric field.
Third, the same aperture lens with a magnetic deflection system for the ion beam, where the magnetic field is extended and the entire beam system is penetrated by that field. This last system is only feasible for small spots and small deflections.

A discussion of the spot size as limited by the aberrations, mainly the chromatic one, follows. Numerical computations of the aberration constants were carried out and have revealed the electric aperture lens as a good candidate with qualities comparable to those of magnetic microscope lenses. Finally, the detection system is quite unconventional in that, owing to the small working distance of a few mm between lens and target and to the large electric field there, secondary charged particles cannot be used for signal generation; instead we use a thin target and measure the time in which the primary ion beam sputters through the target. By this means, we focus, align, and adjust the optical corrections. - But first it is necessary

to say what we mean by brightness and what one may expect in the way of emission current densities from FI or FE tips and sputter removal velocities at the target.

II. Brightness and Speed of Sputtering

For a quasi point source, the brightness ß at some position along the beam is simply the beam current divided by the cross sectional area and divided by the solid angle Ω, within which current arrives into each element of the cross section. The brightness changes proportionally to the beam potential U and one can define a chromatic brightness $ß_c = ß/U$. $ß_c$ is invariant along the optical system of the beam provided that there are (1) no space charge effects and (2) no aberrations of the optical elements. We have no space charge effects in the present case, because 10^{-10} A at 30 keV means ions follow each other at distances of 0,1 mm, a distance larger than the probe diameter. Aberrations however, will reduce the $ß_c$ values at the target by a large factor.

The brightness at the source is more difficult to deduce. For a Maxwellian energy distribution function and an angular distribution following the cosine law, Langmuir[3] has found that $\Omega = \pi$ and $U = kT/e$, so that simply $ß/U = \pi j_e/kT$ with j_e the emission current density.

FI sources emit from a spherical shell in front of and a small distance away from the spherical tip surface[4]. The transverse energy distribution corresponds to the gas temperature. There is also a potential change through the shell thickness of about 1V and a corresponding spread in the axial energy of the beam. This determines the chromatic aberrations, but not the brightness (as evidenced by the agreement of the measured ion microscope resolution at liquid He temperatures with the theoretical resolution[5]. FI sources of heavier noble gases[6] may emit as much as j_e = 10 to 100 Acm^{-2} and thus have chromatic brightnesses at room-temperature of $ß_c$ = 300 to 3000 $Acm^{-2}sr^{-1}\ eV^{-1}$. This compares favorably with values quoted by H. Liebl[1] for the duoplasmatron source of ß = 100 to 200 $Acm^{-2}sr^{1}$ at 12keV or $ß_c$ = 8 to

16 mA $cm^{-2}sr^{-1}eV^{-1}$. Somewhat higher values were recently reported by Drummond and Long[7].

There is also the phenomenon of field evaporation (FE), where the emitting surface is the tip surface itself. Measurements of j_e were made in pulsed operation[8] and they indicate some $10^5 Acm^{-2}$. There are also continuously operating liquid metal FE sources[9] with hints that the j_e-values are even higher. Although there are no measurements, one may expect a narrower axial energy spread than in the case of FI.

The speed of sputtering at the target is equal to the current density j_t times the sputtering efficiency - very roughly one particle per incident ion. What j_t-values can be expected? This depends on the solid angle Ω_t, the beam potential U_t, and the brightness loss factor due to lens aberrations, L.

$$j_t = \beta_c U_t L \Omega_t$$

To limit the effects of the aberrations, Ω_t must be kept small or around 1 mrad or 3 μsr. This leaves us with j_t in the Acm^{-2} range compared with some $mAcm^{-2}$ for the ordinary source. The sputtering speeds are then 10^4 monolayer per second or $3\mu m\ sec^{-1}$. A 300 Å thick target would be cut through in 10 msec.

III. Ion Optical Arrangements; the Aperture Lens.

The three arrangements which we contemplated are shown in the first slide (Fig. 1):

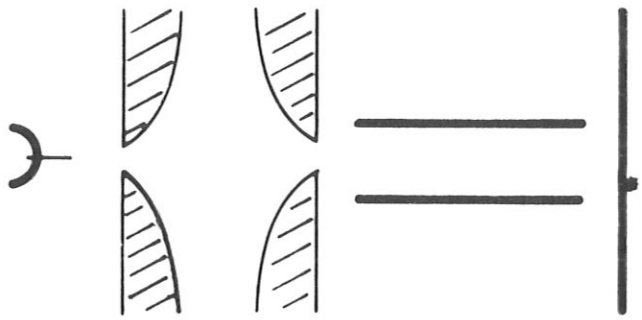

Fig. 1a

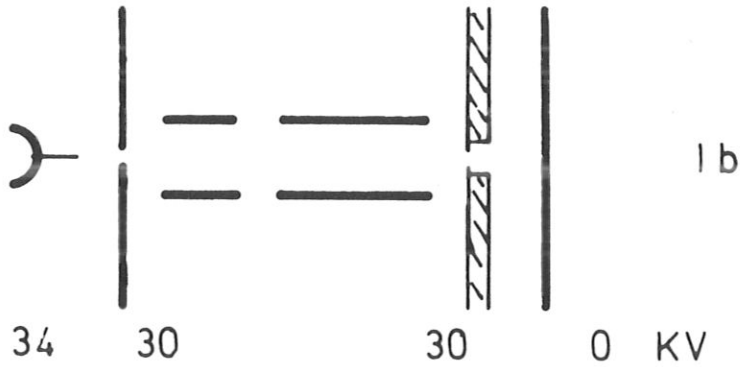

1b

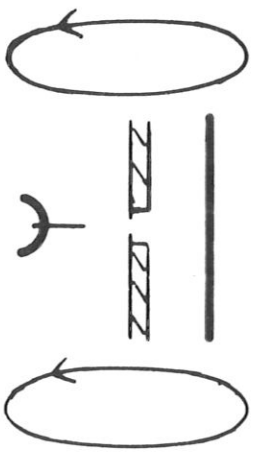

1c

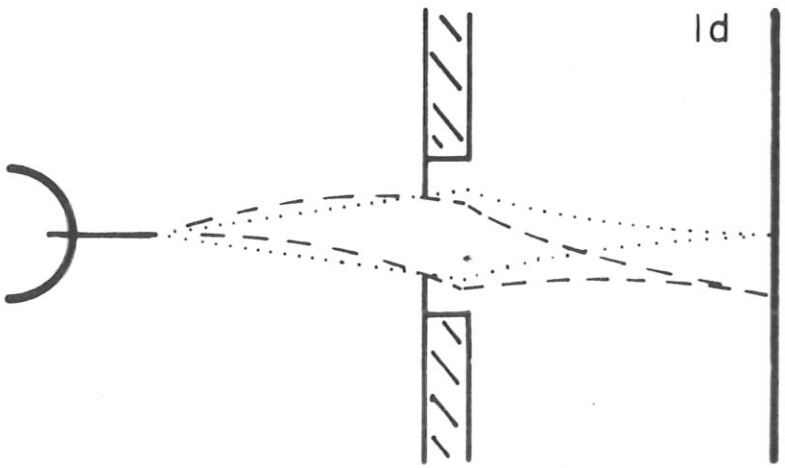

1d

Fig.1: Beam formation and scanning systems; at left the field ionization tip and accelerating electrode;

a) lens and deflection system according to ref. 2;
b) electric deflection system followed by an electrostatic immersion lens, the design used in this paper;
c) same as b), but the electrical deflection system omitted, deflection obtained by extended, externally applied, magnetic coil system;
d) trajectories for case c), undeflected:dotted, deflected:dashed lines, angles exaggerated.

a) from left to right: the FI tip, a non-limiting aperture, an accelerating lens with the limiting aperture at the second electrode, an electric deflection system, and the target; both the special lens and the deflection system are described in ref. 2.

b) Here, the beam is deflected prior to entry of the lens in a deflection system similar to the one in a), except that a return deflection is provided by a second system in order to change the angle of incidence to the center of the last lens. The variation of the position of the beam occurs at the focus of the lens. This is the design used in scanning electron microscopes, except that those deflection systems are magnetic. The lens - the electric aperture immersion lens - will be discussed below.

c) This arrangement is identical to b), except that the deflection system is omitted. Instead, deflection is obtained by a magnetic field applied from outside the electric fields of tip and lens or even outside the vacuum system. Even though these are heavy ions and the entire ion trajectory is less than 10 mm long, enough deflection can be effected with a field of 100 G to deflect about a mrad or a few microns at the target and to do this with modest power in the coils. This scheme is only for very high resolution. Owing to the very small deflection angles, deflection aberrations also remain small. In part d) of the figure we show the envelopping trajectories for an undeflected and a deflected ion beam. All angles are exaggerated.

We have constructed the system b) only. Following the design of Fig. 3 of ref. 2, the deflection system has twice the eight deflection plates to permit correction for astigmatism.

The aperture lens is unconventional for microscopes. It consists of an aperture with an electrical field at the image side and zero field at the object side. The focal length of such lenses, if large compared to the opening, is independent of the target

distance and of the aperture diameter. For focus at the target the target potential U_t should be 9 times the potential U_L, with which the beam enters. For the object not at infinity, but closer to the lens as it is drawn in case c), the voltage ratio U_t/U_L must be greater than 9. U_L being fixed as the voltage required to draw the field ions, e.g., 4 kV, one needs rather high target voltages. This is one of the disadvantages of the lens. A second disadvantage is the fact that the target surface is exposed to the high electric field of the lens, a fact which demands much care in the design of the target holder. But there are important advantages to this lens in comparison with the electrostatic einzel lens. For the same final energy and limited by vacuum breakdown, the aperture lens gives the shortest focal length possible, namely the safe breakdown distance between two parallel planes, Along the optical axis of the aperture lens only forces directed toward the axis are experienced, whereas the einzel lens has first away-from-the-axis and then toward-the-axis forces. Hence, the spherical aberration constant C_s is smaller. In the following discussion of the spot size, we shall first report on some properties of this lens.

IV. Spot Size as Limited by Lens Aberrations

For the aperture lens[10] the electric potential can be written analytically[11] and one can therefore program a computer to calculate C_s and C_c.

The determination of the spherical aberration constant from trajectory calculations is best carried out in the following way. Use the equation $\delta_s = C_s' \alpha_o^3$ as definition for C_s'

$$C_s' = \delta_s \alpha_o^{-3} \qquad (1)$$

δ_s and α_o are defined in the next slide (Fig. 2). Only rays in the immediate vicinity of the focal points F and F' have to be

considered. They are essentially straight lines like in equipotential lenses. Therefore, the diameter of the disc[12] of minimum confusion[13] due to the aberrations is

$$\delta_s = \frac{1}{2} \alpha_o \Delta f \tag{2}$$

In the calculations, we vary the axial distance r from which we start trajectories in the field free side of the lens and parallel to the axis. The calculation furnishes both $\alpha_o(r)$ and $\Delta f(r)$. In the limit of $r \to o$ one observes

$$\alpha_o (r) = Ar \text{ and } \Delta f(r) = B r^2 \tag{3}$$

hence $2\delta_s = AB r^3$. Substituting (2) and (3) into (1), yields

$$C_s' = \frac{1}{2} B/A^2 \tag{4}$$

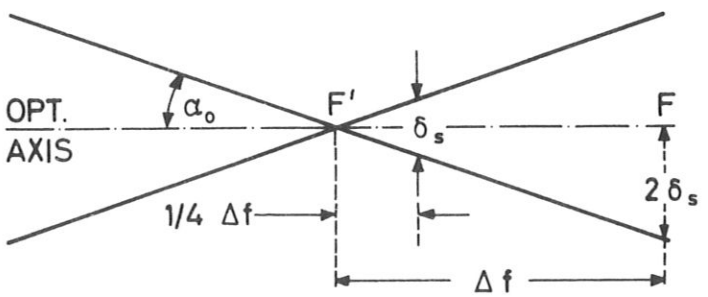

Fig. 2: Region around the main focal point F and the focal point F', changed from F by Δf due to spherical aberration; α_o angle of the peripheral ray with optical axis; δ_s diameter of disc of minimum confusion.

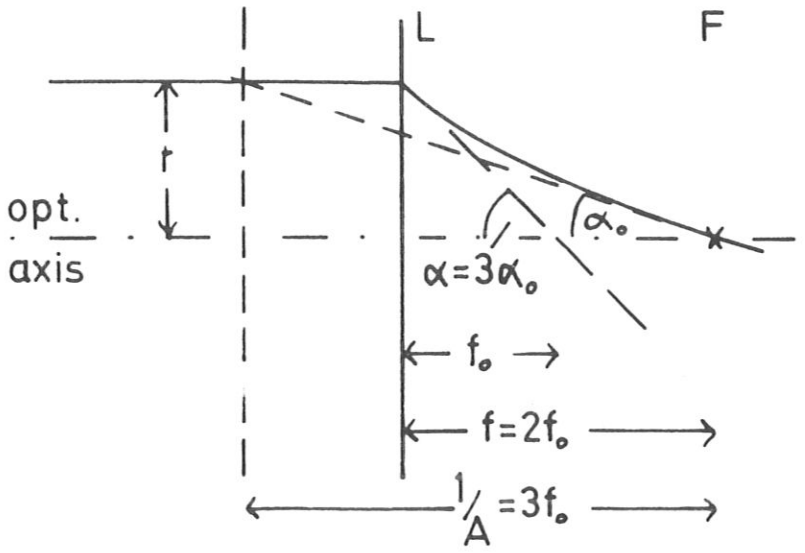

Fig. 3: For the thin aperture lens, relations between theoretical (as if there were no acceleration) focal length f_o, the actual focal length f and the focal length 1/A (equ.(3)); L lens, F focal point, r axial distance (exaggerated); the half angle α_o at F is one third the theoretical half angle α.

In order to relate C_s' to the C_s values of electrostatic einzel lenses, we have to refer the half angle to the focal length f_o, with which one describes the optical lens properties like magnification and the object-image-distance relation.[14] The C_s' in equ. (1) should refer to $\alpha = 3\,\alpha_o$ rather than to α_o and

$$\delta_s = C_s' \alpha_o^3 = \frac{1}{27} C_s' \alpha^3 = C_s \alpha^3, \quad \text{or}$$

$$C_s = \frac{1}{27} C_s' \qquad (5)$$

In the next slide (Fig. 4) we plot C_s as a function of f_o and present in the same figure a comparison with the electric einzel lens from ref. 12 p.38. The immersion lens shows a lower spherical error than the einzel lens. Especially at the shortest

focal lengths, the ratio $C_s/f \approx 1$ for this lens compared to 10 for the einzel lens (Ref.12, p. 308)

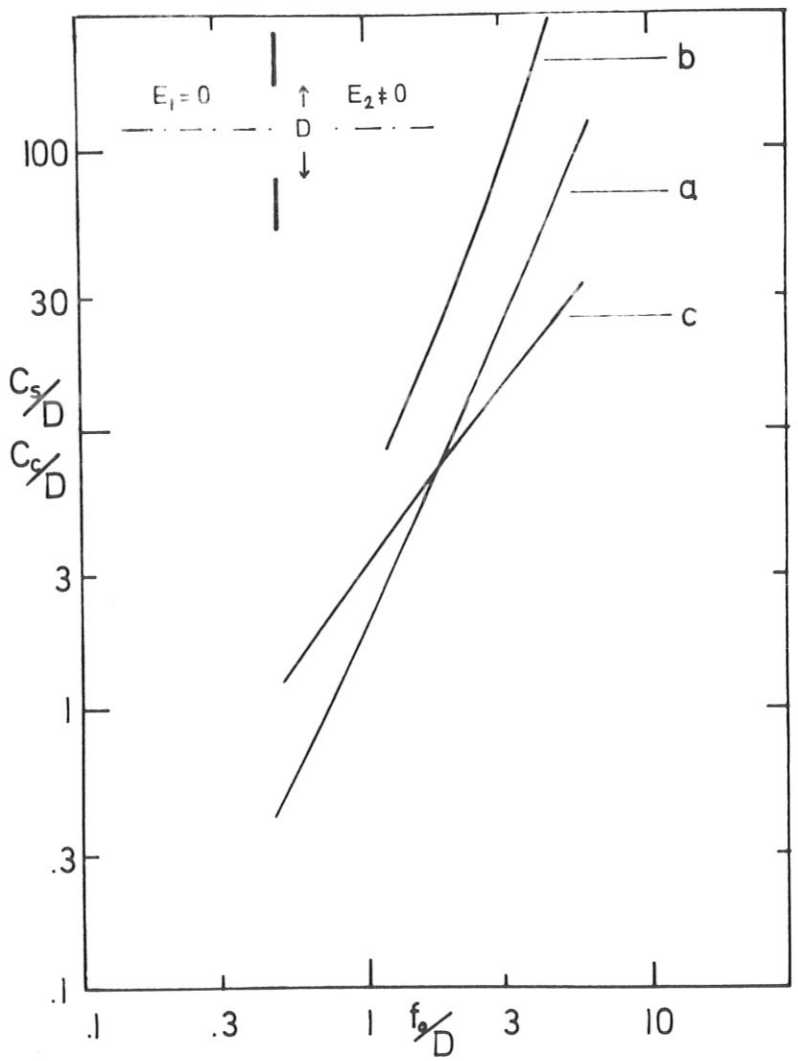

Fig. 4: Spherical and chromatic aberration constants C_s and C_c for the electrostatic aperture lens ($E_1 = 0$, $E_2 \neq 0$ and aperture diameter D) versus the optical focal length f_o used here.
a) results of trajectory computation for C_s
b) C_s for the electrostatic einzel lens from ref.12 p.38
c) results of trajectory computation for C_c.

The determination of the chromatic aberration constant from trajectory calculations is carried out in the following way. Again, we use as definition of C_c the relation $\delta_c = C_c \alpha \ \Delta U/U_t$, where U_t refers to the potential at the focal position (target) and ΔU is the variation in the initial energy of the particles. δ_c is computed from the focal length change Δf with ΔU and from α_o by equ.(2). Using the thin lens relation $\alpha = 3\,\alpha_o$ one obtains

$$C_c = \frac{\delta_c U_t}{3\,\alpha_o\,\Delta U} \qquad (6)$$

Values of C_c/D vs f_o/D are entered in Fig.4 as curve c. The immersion lens shows about the same chromatic error constant as the einzel lens. The ratio $C_c/f = 3.5$ for this lens is to be compared with 4 for the einzel lens.

Generally, for the aperture lens the spherical aberration and the focal length are smaller than those of the einzel lens. They are more comparable to the typical magnetic lenses for microscopes (ref.12,p.303). The chromatic aberrations are not smaller and not comparable to those for magnetic lenses.

For small δ-values, one has to use the lowest possible f/D-value compatible with electrical breakdown distances. For $f/D < 1$, one enters the regime of a thick lens, for which the relation $f = 2\,f_o$, and $\alpha = 3\,\alpha_o$, and $U_t = 9U_L$ do not hold any more. Nor is the function for the potential of ref. 9 correct, because the target is not an equipotential plane anymore. This can be remedied by adding an identical, but mirrored potential, which enforces a plane equipotential at the target position. For these more practical conditions we plan individual numerical calculations.

In order to estimate the various contributions to the probe diameter δ, we use a lens with $U_L = 4$ kV, $U_t = 36$ kV, $D = 2$ mm, $f_o = 2{,}5$ mm, $f = 5$ mm, $C_s = 6$ mm, $C_c = 8$ mm. It is customary to compose in quadrature:

$$\delta^2 = \delta_i^2 + \delta_s^2 + \delta_c^2 + \delta_d^2 \qquad (7)$$

where the spot diameter δ_i is solely due to the image size, δ_s due to spherical, δ_c due to chromatic, and δ_d due to diffraction aberrations. In the optical arrangement b of Fig. 1 we have an object distance of 50 mm, hence a size reduction of $\approx 1 : 20$. The apparent object size from an emitter tip of radius 400 Å after acceleration to 4 kV with thermal initial transverse energy of 0.4 eV is 8 Å [15] and the image size $\delta_i = 0.4$ Å.

δ_s, δ_c, and δ_d are functions of the half angle α and are taken respectively from $\delta_s = C_s \alpha^3$, $\delta_c = C_c \alpha \cdot \Delta U/U_t$, and $\delta_d = 0.6 \lambda/\alpha = 5 \cdot 10^{-4}/\alpha$ Å. In the next slide (Fig.5), we plot the three diameters in Angstrom units versus α in mrad (ref.12,p.293). Note that the optimum angles α at 0.3 and 0.5 mrad are mainly determined by the chromatic aberrations. The comparable graph for electrons shows much larger minimum δ's, because of the larger diffraction effect.

The current density in the spot is of primary interest. There arrives at the spot only the current corresponding to the aberration-free image size δ_i, namely $4/\pi \cdot \delta_i^2 j_t$. This current is spread over $\pi/4 \cdot \delta^2$ with the loss of brightness given by

$$L = \delta_i^2 / (\delta_i^2 + \delta_s^2 + \delta_c^2 + \delta_d^2) \qquad (8)$$

With $\delta_i = 0.4$ Å, we find at $\alpha = 0.5$ mrad, that L is only 8 %. In order to better match δ_i with δ, we have thought of the arrangement c of Fig. 1, the one with magnetic deflection.

The measurement of probe currents and sizes is difficult, because the target is located in the electric lens field and the working distance is quite small. Instead of using a secondary ion or electron or X-ray signal, we use the primary beam in transmission. Since the range of ions in the target is small, but the removal rate of target material is large, we use thin targets and measure

"sputter-through times". These times indicate the degree of focus and can be directly related to the target current densities.

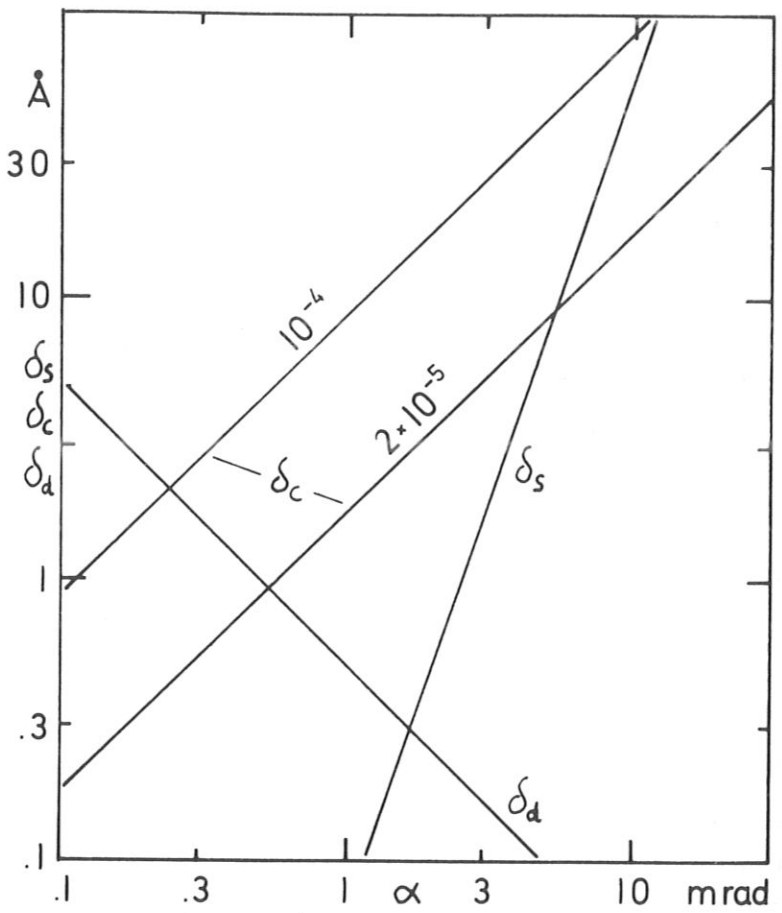

Fig. 5: Three contributions to the final probe diameter δ in Angstrom units: δ_s due to spherical aberrations, δ_c due to chromatic aberrations, and δ_d due to diffraction, all three as function of the half angle α of the beam in mrad; δ_c for $\Delta U/U = 2\cdot10^{-5}$ and 10^{-4}; C_s = 6 mm, C_c = 8 mm, $\lambda = 5\cdot10^{-4}$ Å for 4 keV and M = 100 ref.18.

V. Conclusions

Ion probes can be made smaller than electron probes because of the smaller diffraction effect. The necessarily electrostatic lenses have larger focal lengths and spherical aberrations constants, than the magnetic lenses for electrons. An exception, however, is the electric aperture lens which involves the complication of having the target in the electric field. Field ionization or field evaporation tips are suitable as bright sources.

Because ions interact more strongly with surfaces, ion probes below 1000 Å in diameter become impractical for surface analysis. They are too destructive. But for the manufacture of small structures, they are well suited.

References

1. H.Liebl, J.A.P. 38, 5277 (1967)
2. A.V.Crewe, M.Isaacson, D.Johnson, Rev.Sci.Instr.40, 241 (1969)
3. D.B.Langmuir, Proc. IRE 25, 977 (1937)
4. E.W.Mueller and Tien Tzon Tseng, Field Ion Microscopy, Elsevier, New York, 1969 p. 17.
5. ref. 4, p.40.
6. For example, E.W.Mueller and K. Bahadur, Phys.Rev.102, 624 (1956)
7. I.W.Drummond and I.V.P.Long, Proc.First Int.Conf. on Ion Sources, Saclay 1969, p. 459.
8. E.W.Mueller, Naturw. 57, 22 (1970) and Quarterly Reviews 23, 184 (1969).
9. D.S.Swatik, Theses, University of Illinois, Urbana, 14 May 1969 and J.F.Mahonney et al., J.A.P. 40, 5101 (1969).
10. V.K. Zworykin et al., Electron Optics and the Electron Microscope, John Wiley, New York, p. 441-447 (1945).
11. F. Ollendorff, Potentialfelder der Elektronik, Berlin 1932, p. 295.
12. M.v.Ardenne, Tabellen der Elektronenphysik, Ionenphysik und Übermikroskopie, Berlin 1956, p. 39.
13. A.B. El-Kareh et al., Electron Beams, Lenses and Optics, Academic Press, Vol. 2, p. 53-55,1970
14. H.Heil, IRE Convention Record, Part III, p.118 (1956) for U_L/U_t values other than 9; and H.Heil and B.W. Scott, Proc. Second Int.Conf. on Electron and Ion Beam Science and Technology; Am. Inst. of Mining, Metallurgical and Petroleum Engineers, New York 1969, Vol. II, p. 974 (1966).
15. E. Ruska, Z. Phys. 83, 684 (1933).